Radio Science, Volume 12, Number 5, pages 821-829, September-October 1977

Spacecraft observations of man-made whistler-mode signals near the electron gyrofrequency

N. Dunckel[1] *and R. A. Helliwell*

Radioscience Laboratory, Stanford University, Stanford, California 94305

(Received September 9, 1974; revised March 21, 1977.)

Whistler-mode signals from low-frequency ground-based transmitters in the 60-100 kHz range are observed by the OGO-1 satellite at frequencies unusually close to the local electron gyrofrequency, f_H. The intensity of signals observed on outbound passes near 40° geomagnetic latitude remains high until the decrease in f_H causes the normalized frequency f/f_H to approach 0.9. Here the signal disappears abruptly into the background noise, a change of at least 20 dB. Ray-tracing calculations provide a simple explanation for the sudden loss of signal. Rays in this frequency range which are launched just inside the plasmapause reach an altitude where $f/f_H \simeq 0.9$ before abruptly bending inward toward the earth's equator. Rays launched outside the plasmapause are reflected in the form of a "Spitze" at the point where the plasma frequency decreases to the wave frequency. Thus the primary features of the observed LF propagation in the magnetosphere can be explained using classical cold-plasma expressions for the refractive index.

INTRODUCTION

The behavior of whistler-mode waves at frequencies approaching the electron gyrofrequency, f_H, is of interest because of the possibility that damping of the waves may occur. Such damping of whistler-mode waves has often been predicted [*Liemohn*, 1967, and references therein] but has not yet been reported. The present study extends the range of whistler-mode wave observations to $f/f_H \simeq 0.9$, where an abrupt cutoff is observed. This cutoff can be explained entirely in terms of accessibility and hence, if there is damping, it must be limited to normalized frequencies above 0.9.

Ground-station observations of whistlers are usually limited to frequencies below $0.5\ f_{Ho}$, where f_{Ho} is the equatorial value of f_H [*Carpenter*, 1968]. The narrow spread of the distribution of observed upper-cutoff frequencies indicates that the cutoff is caused by the loss of ducting at $0.5\ f_{Ho}$ as suggested by *Smith* [1961]. Satellite-borne receivers, which extend the observations to nonducted signals, show the presence of whistler-mode signals at higher frequencies relative to the gyrofrequency. Using the OGO-3 satellite, *Angerami* [1970] has observed whistlers at frequencies as high as 0.7 f_H. These whistlers had apparently leaked from ducts as their frequency increased above $0.5\ f_H$.

Signals from ground-based transmitters operating near 18 kHz have been studied by *Heyborne* [1966, pp. 111-202] using the OGO-1 satellite. Transmissions were generally observed from low altitudes out to the region where f/f_H decreased to ~0.3, which on outbound passes occurred in the vicinity of 30° to 40° geomagnetic latitude. A slow fadeout rather than a sudden cutoff was commonly observed. After the fadeout there sometimes occurred brief, occasionally intense, recurrences of the signal. It is likely that these were due to ducted signals encountered by the satellite.

In contrast to the slow fadeout of the 18 kHz signals at $f/f_H \simeq 0.3$, the 60-90 kHz waves discussed here often remain strong until f/f_H reaches ~0.9, where they exhibit an abrupt cutoff in intensity. Heyborne's analysis suggests that the difference in behavior results from the difference in locations of the respective transmitters. The 60-90 kHz transmitters are located relatively close to the entrance point in the ionosphere for rays reaching $f/f_H \sim 0.9$, while the 18 kHz transmitters are at lower latitudes. Thus propagation losses in the earth-ionosphere waveguide may account for the fading out of the 18 kHz signals at relatively low values of f/f_H.

An implication of this study is that fairly specialized conditions are required in order for a wave in the magnetosphere to reach normalized frequen-

[1]Present address: ESL, Inc., 495 Java Dr., Sunnyvale, California 94086.

cies as high as $f/f_H \sim 0.7$. Thus throughout much of the magnetosphere the frequency range $0.7\ f_H < f < f_H$ is characterized as being electromagnetically quiet.

THE EXPERIMENT

The low-frequency radio-wave experiment on OGO-1 covered the frequency range 0.2 to 100 kHz with three stepping receivers and a fourth broadband receiver which processed waveforms of signals in the 0.2 to 13 kHz range for transmission to the ground. Signals were received by a loop antenna and preamplifier common to all receivers. The data used in the present experiment came from the highest-frequency stepping receiver which covered the range 12–100 kHz in 256 steps over a period of 2.3, 18, or 147 sec, depending upon the telemetry rate. The 3 dB bandwidth of the receiver was 600 Hz. Data from the stepping receivers were processed so that complete sweeps could be photographed on consecutive frames of 16 mm movie film. Further details concerning the experiment can be found in *Dunckel and Helliwell* [1969] and the references therein.

DATA

On outbound passes of OGO-1, man-made transmissions appear in the 12–100 kHz spectra as narrow spectral lines. These may be differentiated from natural noise by the invariance of their frequency, by the relative constancy of their intensity with time, and by their narrow bandwidth. From the intensity of the signal in the spectra displayed on consecutive frames of 16 mm movie film, a graph of intensity vs. time can be developed. Figure 1 shows an example of the intensity of transmissions at 74 kHz obtained in this way during an outbound pass of the OGO-1 satellite.

The time between samples is initially 18 sec; after 0316 UT it decreases to 2.3 sec. Data points for these later data were obtained by averaging eight data points together and consequently they show somewhat less fluctuation than the previous data. Amplitudes are shown in terms of db above 1 micro-gamma in the 600 Hz receiver bandwidth; thus 20 dB represents a field strength of 10^{-5} γ. The ratio of signal frequency to the local electron gyrofrequency, f/f_H, appears at the top of the figure. The position of the satellite during this pass is shown in the upper right-hand part of the figure; at the satellite the local time is midnight.

Of interest here is the sharp decrease in intensity by 15 dB to the background level that occurs from 0316 to 0318 UT. This decrease occurs when the ratio f/f_H increases from 0.84 to 0.95. The other fluctuations appear to be mostly random except

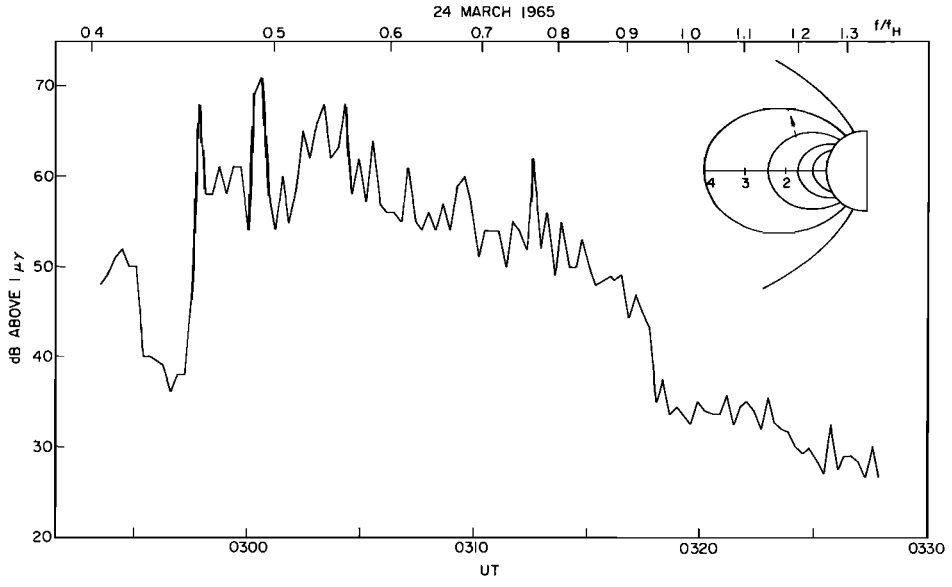

Fig. 1. Strength of 74 kHz signal measured on outbound pass. Satellite location in magnetic meridian plane is shown in inset by dotted line. Note relatively strong signals persisting until $f/f_H = 0.9$, when abrupt fade to background level occurs.

for the sharp depression in intensity occurring at 0255-0257 UT, when the satellite is at $L = 2.0$, magnetic latitude = 18°. A simultaneous decrease occurs in the intensity of man-made signals from 20 to 70 kHz, with the lower-frequency signals being less affected than the higher. The intensity of whistler-mode signals in the range 3-12 kHz also decreases, as indicated by the output of another stepping receiver (not shown). Thus the effect appears to be a propagation effect rather than an interruption of transmissions. The cause may be ionospheric absorption caused by a brief enhancement of D-region ionization [*Helliwell et al.*, 1973]. At low frequencies ($f < f_H$) ionospheric absorption increases with frequency.

After the signal has faded out at 0318 UT, the background level decreases in intensity until about 0325 UT. This change in the background level is often observed and has been identified with the change in spacecraft interference at the location of the plasmapause (N. Dunckel, unpublished manuscript, 1974). In the examples of Figures 1 and 3 this change in the background level was observed shortly after the abrupt decrease in signal intensity.

The track of the subsatellite point across the earth for this example is shown in Figure 2, where the indicated geomagnetic coordinates are based on a simple dipole approximation to the geomagnetic field. Universal times are shown near the end points; tick marks every 5 min show the progress of the satellite. Also shown is the intersection with the surface of the earth of the field line passing through the satellite as computed using the harmonic expansion of the field as given in the satellite ephemeris. This intersection is approximately the location of the entrance into the ionosphere for waves reaching the satellite.

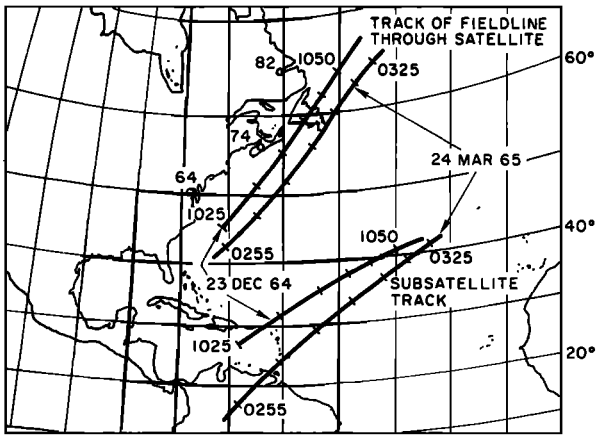

Fig. 2. Map in geomagnetic coordinates of track of subsatellite point and endpoint of magnetic field line passing through the satellite for two separate satellite passes. Tracks are identified by UT near endpoints and by tick marks every 5 min. Transmitting station locations are shown by circles with two-digit numbers representing frequency in kHz.

The locations of transmitters believed to be responsible for the signals shown in Figures 1 and 3 are identified in Figure 2 by the numbers 64, 74, and 82, which represent their frequencies in kHz. These locations were obtained by identifying transmitters operating close to the observed frequency and lying within eastern North America [*International Telecommunication Union*, 1971]. At other frequencies (70 and 97 kHz) there are several possible stations that could have transmitted the observed signals; only transmitters having unambiguous locations are shown.

Another example of signals observed on an outbound pass at frequencies close to f_H appears in Figure 3. Here signals from five transmitters were monitored. Each data point represents the intensity at the indicated frequency scaled from spectra recorded at intervals of 2.3 sec. Note that the data were plotted on a common linear scale of f/f_H. Consequently each frequency has a different time scale as shown in the figure, where the numbers represent minutes after 10 hours UT. The inset shows the path of the satellite in the magnetic meridian plane; the local time at the satellite is 7 to 8 hours. The 70, 74, and 82 kHz signals remain strong until a sharp decrease of about 20 dB to the background level occurs at $f/f_H = 0.86$, 0.92, and 0.93, respectively. The signals at 64 and 97 kHz fade out at lower values of f/f_H.

The behavior of the intensity of the Figure 3 signals prior to the cutoff may be understood qualitatively with the aid of Figure 2. The closest approach of the field-line track to the 64 kHz station occurs near 1025 UT. The intensity record shows that the signal strength reaches maximum at this time and decreases shortly thereafter. Similarly the 74 kHz signal is strongest at 1034 UT when the field-line track is closest to the station. In contrast, the strength of the 82 kHz signal stays constant from 1034 to 1040 UT despite increasing magnetospheric path length, probably due to the decreasing distance from the field line to the station.

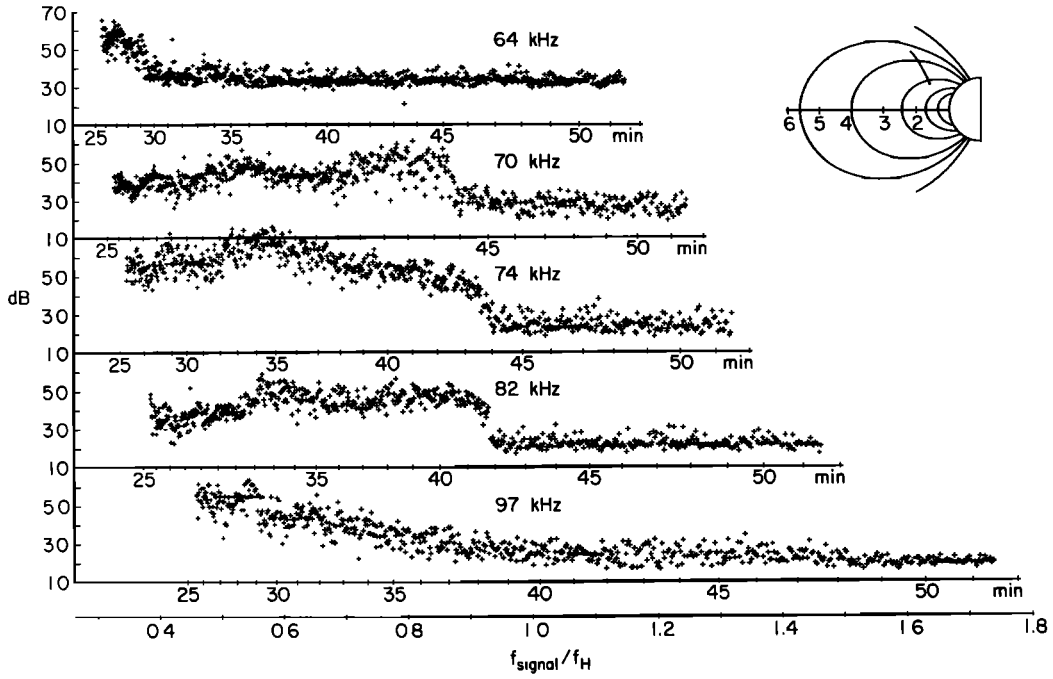

Fig. 3. Strength of signals received on one outbound pass from transmitters at five different frequencies. Vertical scale represents dB above 1 μγ. Time scales, shown in minutes after 10 hours UT, have been distorted to permit the use of a common scale of f/f_H. Note that strength of signals at middle three frequencies remains high until f/f_H reaches 0.87 to 0.92.

These observations suggest that the 70 kHz station is in Newfoundland: several stations operating at frequencies close to 70 kHz are in fact situated there.

The abrupt decreases in signal levels for the three middle frequencies each take place in about one minute. This abrupt decrease in the intensity can be explained by the ray tracings described later.

Examination of about 40 outbound passes shows that transmissions at frequencies up to 0.85 f_H from several of the same stations described above have been observed on three other passes. Two of these passes occurred near midnight local time and one near 7 hours local time; all occurred over the eastern coast of Canada. The observation of the signals close to the gyrofrequency is thus not an isolated phenomenon. The events are characterized by magnetic conditions that were mildly disturbed during the 24 hours previous to the observation (maximum $Kp \simeq 4$ over the previous 24 hours). This level of disturbance is indicative of a plasmapause position of $L \sim 4$ [*Carpenter*, 1967]. It is possible that this location of the plasmapause favors the propagation of these low-frequency waves to high altitudes. The lack of other examples is probably due to the absence of suitable low-frequency transmitters at high magnetic latitudes.

RAY TRACINGS

In an attempt to explain the behavior of the signal intensity, ray tracings were carried out at 80 kHz. Ray paths commencing with vertical wave normals at 1000 km altitude are shown in the magnetic meridian plane in Figure 4 at initial latitudes (at 1000 km) of 50, 55, and 58 degrees magnetic. Emanating from the rays are "wave-normal" vectors whose direction is that of the normal to the wave front and whose length is a nonlinear function of the magnitude of the refractive index. Field lines are shown at $L = 2.0$ and 3.9, the latter representing the inner boundary of the plasmapause as discussed below. The satellite path on 23 December is shown for the time interval 1035 to 1045 UT with tick marks each two minutes.

The electron density model used in the ray tracing

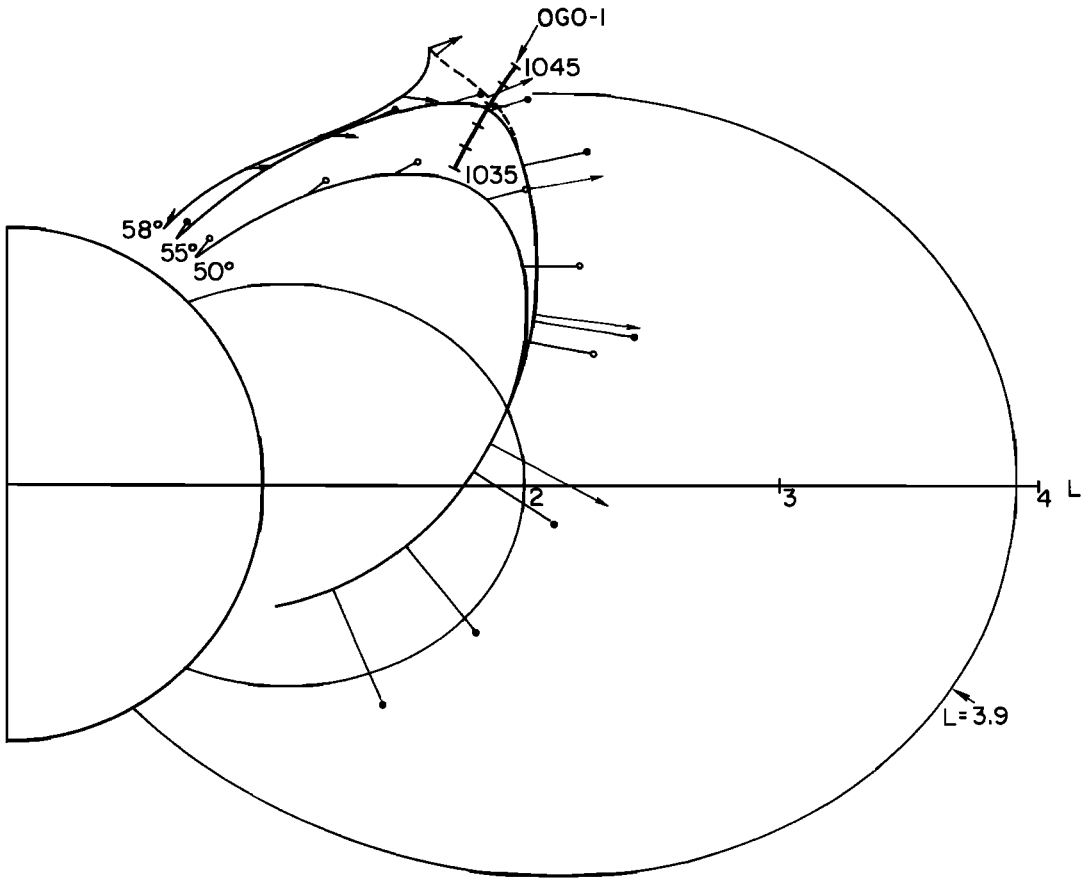

Fig. 4. Ray tracings at 80 kHz to simulate observations shown in Figure 3. Rays commence at 1000 km altitude at magnetic latitudes of 50°, 55°, and 58°. Wave-normal directions are shown by vectors terminating in circles and arrows. Dotted line shows path of ray reflected at plasma frequency. Satellite track in magnetic meridian plane is shown with tick marks every 2 min.

includes a plasmapause whose location and extent has been adjusted to match that indicated by the change in background noise level which occurs at the plasmapause (N. Dunckel, unpublished manuscript, 1974). This change occurred at 1045–1048 UT at 100 kHz and ~1050 UT at 80 kHz. To match these data, a broad plasmapause with an inner boundary at $L \simeq 3.9$ was defined to have plasma frequencies at the satellite equal to the frequencies at which the inflections in background intensity were noted. The resulting electron density model is described in appendix A and is shown in equatorial profile in Figure 6. (A more detailed examination of the change in background level at the plasmapause has subsequently indicated that the plasmapause may actually be more abrupt than indicated. However, the present model closely resembles our best estimate of the location and extent of the plasmapause. Any refinement of this model is unlikely to seriously alter the results presented here.)

The ray commencing at 50° latitude reaches a relatively low altitude before turning inward toward the earth and does not extend to the region where the actual cutoff of the 82 kHz signal was observed at 1042 UT. As the satellite progresses outward, it intersects rays launched at progressively higher latitudes. The ray commencing at 55° latitude would be observed by the satellite at 1041 UT, near the location where the fadeout of the 82 kHz signal occurred. Rays launched at latitudes of 55.5° or higher do not curve back toward the earth but are reflected when the wave frequency becomes equal to the plasma frequency, as shown by the ray

commencing at 58°. The dotted line in Figure 4 indicates the path of the reflected ray. This reflected ray comes closer to the location where the 82 kHz signal was last observed than does the ray launched at 55°. However, it is not clear that any reflected signal is received by the satellite. The fact that the wave faded out at latitudes higher than reached by the 55° ray could easily result from differences between the density model employed in the ray tracings and the actual densities at the time of observation.

An interpretation of the ray tracing calculations based on Snell's law construction [*Helliwell*, 1965, pp. 36-40] has been worked out from a study of ray tracings computed both with and without a plasmapause. The ray path commences at 1000 km altitude where the refractive index surface is identified by $f/f_H = 0.096$ in Figure 5. This figure shows the sequence of refractive index surfaces for the locations designated in Figure 4 by the first five wave-normal vectors on the 55° ray. Each graph is a polar diagram in which the radius indicates the magnitude of the refractive index μ at the angle θ, the wave-normal angle, from the static magnetic field. The normal to the refractive index surface at any point (μ,θ) indicates the direction of the ray identified with that refractive index vector. An arrow indicates the ray direction for each of the surfaces; the refractive index vector is shown only for the bottom-most surface.

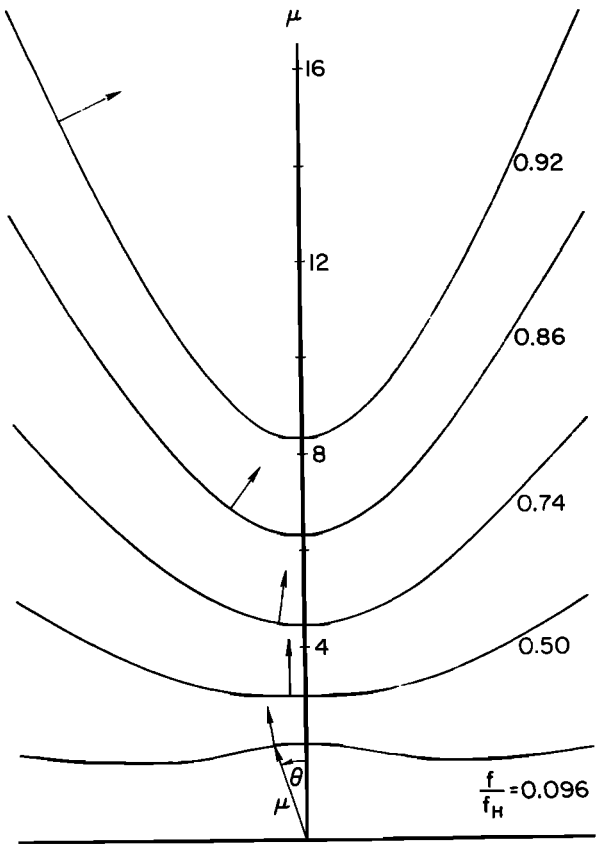

Fig. 5. Refractive index surfaces for ray commencing at 55° in Figure 4. Vertical axis is direction of earth's magnetic field. Arrows above surfaces show ray direction. The wave-normal vector, at the angle θ, is shown only for the lowest surface. Change in geometry of surface at large values of f/f_H forces ray direction to become nearly perpendicular to the magnetic field.

For rays launched inside the plasmapause with vertical wave normal angles, such as the one commencing at 55° in Figure 4, the decrease in electron density is more than offset by the decrease in gyrofrequency as the wave moves upward so that the refractive index increases. The gradient of refractive index initially points about 50° equatorward of the direction of the static magnetic field $\bar{B}_0$. This causes the wave-normal angle to decrease, but very slowly. The change in the topology of the refractive index surface at $f/f_H \simeq 0.5$ (see Figure 5) then causes the ray to swing toward the equator. The decreasing gyrofrequency causes the resonance cone to contract, with the result that the ray rapidly approaches the perpendicular to the magnetic field. At this time the ray turns sharply toward the earth.

Rays traveling in the vicinity of the plasmapause, such as the ray shown in Figure 4 launched at 58°, have wave vectors that move rapidly from poleward of $\bar{B}_0$ to equatorwards of $\bar{B}_0$. This results from the domination of the refractive index by the rapid decrease of electron density with altitude outside the plasmasphere together with the large cross-L density gradient. These rays move inward to lower L values until the decreasing gyrofrequency deforms the refractive index surface such that the ray direction points outward. These rays then curve outward through the plasmapause to higher L values until they reach the point at which the plasma frequency, f_p, decreases to the wave frequency. The behavior of whistler-mode rays near the point at which $f_p = f$ has been discussed by *Budden* [1966]. Although the wave mode is different, the ray path at reflection is essentially the "Spitze" described by Budden. As the wave moves outward, the refractive index surface collapses into a line

parallel to the earth's magnetic field $\bar{B}_0$. We assume the gradient of refractive index to be essentially that of the gradient of electron density, which is nearly perpendicular to $\bar{B}_0$ due to the large electron density gradient in the vicinity of the plasmapause. As f_p approaches f, the ray direction changes abruptly by 180°. (In practice the reflection was computed at the point where the angle of the resonance cone was 1°. As a check, essentially the same ray path was found when the reflection was computed at the point where the angle of the resonance cone was 5°.) The reflected ray begins with its ray direction anti-parallel to the incident ray and then diverges to move to higher altitudes. The reflected ray, shown by the dashed line in Figure 4, then joins the trajectory of the 55° ray.

That the wave is reflected rather than transmitted at $f = f_p$ can be understood from Snell's law. The medium is stratified in planes almost parallel to $\bar{B}_0$, and the wave-normal angle is close to 0°. The refractive index for the incident wave remains virtually constant at 4.3 as the ray approaches the reflection point. Since the refractive indexes for the transmitted mode at $f > f_p$ are less than 2.2, there can be no transmitted component.

DISCUSSION

Reflection at the plasma frequency can occur for LF rays starting at latitudes from 55.5° to at least 60°. Within this range, rays starting at the lowest latitudes reflect at the highest altitudes. Although ray tracings have been carried out only for the example shown in Figure 4, it appears likely that the paths of other reflected rays merge into the 55° ray in a manner similar to the reflected ray shown.

It is not clear whether the existence of the reflected ray is confirmed by the data in Figures 1 and 3. The fact that the signals were observed slightly longer than indicated in Figure 4 by the ray commencing at 55° suggests the existence of the reflected wave. However, the discrepancy is small and may well be caused by minor differences between the actual and modeled conditions. Observations from low-altitude satellites indicate that waves near 20 kHz do not propagate up to the satellite in the region around the plasmapause [*Heyborne*, 1966, pp. 169–171; *Heyborne et al.*, 1969]. Thus it is uncertain whether or not the reflected wave actually exists.

The ray tracings shown in Figure 4 give a very satisfactory explanation for the observed cutoff of the signals. The fact that this relatively simple model accounts for the observed behavior of the signals does not, of course, rule out the possibility that the actual behavior of the rays is more complicated. For instance, similar results could probably be obtained by assuming that the signals are initially ducted at a location just inside the plasmapause and then become unducted as they travel to regions where $f/f_H \geq 0.5$. The confinement within the duct might allow the ray to reach slightly higher values of f/f_H than do the rays considered here. Although such ducting is not required to explain the present observations, further examination of the OGO-1 and OGO-3 data might indicate whether such ducting actually occurs.

The behavior of the rays shown in Figure 4 is not limited to frequencies near 80 kHz. Ray tracings carried out for a density model similar to that described here show that 16 kHz waves launched at a latitude of 60° reach ratios $f/f_H \simeq 0.98$. The rays reach these high ratios as a result of being refracted by the plasmapause at lower altitudes. The ray paths are similar to those shown by Alexander (unpublished manuscript, 1971) for 16 kHz rays.

No man-made signals in the 14–25 kHz range have actually been observed so close to the gyrofrequency despite extensive observations in the regions where they should occur. This fact may be related to the previously mentioned absence of waves in this frequency range at low latitudes just outside the plasmapause, or may be due to the absence of transmitters in this frequency range at high latitudes.

The reflection exhibited in Figure 4 by the ray starting at 58° is limited to rays which reach the plasmapause before the angle between the wave normal and the resonance cone becomes too small. Rays launched at latitudes much greater than 60° will, like the 55° ray, bend inward toward the earth. As long as the ray is well outside the density gradients associated with the plasmapause, there is no outward refraction (as with the 58° ray) and hence no reflection. When the ray does reach the plasmapause, the wave normal angle is sufficiently close to the resonance cone that the density gradient is unable to refract the wave, and the ray passes into the plasmasphere.

We conclude that the primary features of LF

propagation in the magnetosphere can be described to first order using the classical expressions of the magnetoionic theory.

APPENDIX A: RAY TRACING TECHNIQUES

The ray-tracing calculations were carried out by a computer program written by *Walter* [1969, pp. 97-108] and modified by *Angerami* [1970]. A simple dipole model of the earth's magnetic field was employed. The magnitude of this field was scaled downward by 5.4% to make the model field agree with that given in the ephemeris for the location of the satellite at cutoff. (The ephemeris field was computed using a harmonic expansion.)

The electron densities are based on a field-aligned isothermal diffusive-equilibrium model [*Angerami and Thomas*, 1964]. The variation of density with L-shell was assumed to be L^{-1}. The temperature was assumed to be 1000 K and the composition to be 80% H^+ and 20% O^+ at 1000 km. The model assumed an electron density of 2800 cm^{-3} at 1000 km.

This model was modified to include a plasmapause by multiplying the diffusive equilibrium electron density obtained at a geocentric distance R and an L-shell L by

$$ANLK(L,R) \equiv \begin{cases} 1, & \text{for } L < LK \\ A + [1 - A][B + (1 - B)C], & \\ & \text{for } L \geq LK \end{cases} \quad \text{(A1)}$$

where

$$A \equiv \exp - [(L - LK)^2/2(DDK)^2] \quad \text{(A2)}$$

$$B \equiv (RCONSN/R)^{EXPK} \quad \text{(A3)}$$

$$C \equiv \exp - [(R - RCONSN)/SCR]^2 \quad \text{(A4)}$$

These variables (and their assumed values) are defined as follows: LK (=3.9 earth radii) is the L-shell of the inner boundary of the plasmapause; DDK (=0.4 earth radii) is the half width of the plasmapause at the equator; $RCONSN$ (=7000 km) is the geocentric distance above which the electron density inside the plasmapause is greater than the density outside; $EXPK$ (=3.0) is the exponent of R by which the electron density is decreased at $L \gg LK$; SCR (=500 km) is a measure of the radial distance above $RCONSN$ at which the electron density becomes significantly affected by the term R^{-EXPK}. The effect of the term $ANLK$ is to provide a smooth transition from the diffusive equilibrium model inside the plasmapause to a model with a more rapid decrease of density with increasing height outside.

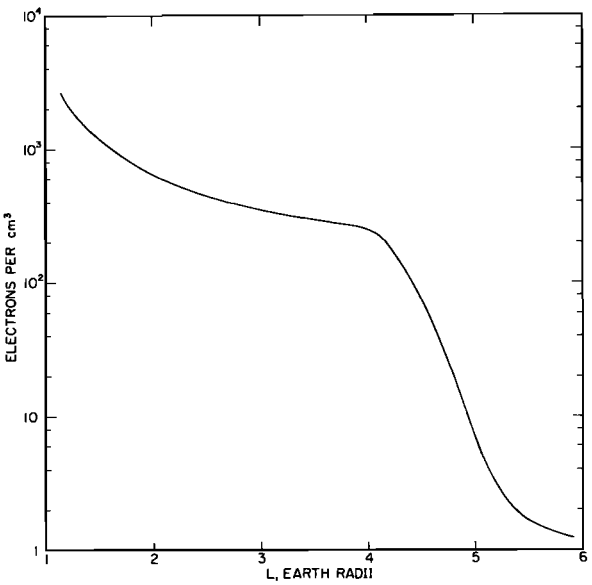

Fig. 6. Model electron density in equatorial plane. A diffusive equilibrium model is used inside the plasmapause and an approximately R^{-4} model outside.

Figure 6 shows the resultant electron density distribution in the equatorial plane. The modified density outside the plasmapause decreases approximately as R^{-4}, a valid model outside the plasmapause [*Angerami and Carpenter*, 1966]. (Note that at $R < RCONSN$ the model is invalid outside the plasmapause as it gives a higher density there than inside. No ray tracings were carried out in this region.)

Acknowledgments. The authors are indebted to J. Angerami for his suggestion that the observed behavior could be explained through ray tracing and for his assistance in carrying out these calculations. This research was funded by the National Aeronautics and Space Administration under grant NGL-05-020-008.

REFERENCES

Angerami, J. J. (1970), Whistler duct properties deduced from VLF observations made with the OGO-3 satellite near the magnetic equator, *J. Geophys. Res.*, *75*, 6115-6135.

Angerami, J. J., and D. L. Carpenter (1966), Whistler studies of the plasmapause in the magnetosphere, 2, Electron density and total tube content near the knee in magnetospheric ionization, *J. Geophys. Res.*, *71*, 711-725.

Angerami, J. J., and J. O. Thomas (1964), Studies of planetary atmospheres, 1, The distribution of electrons and ions in the earth's exosphere, *J. Geophys. Res.*, *69*, 4537-4560.

Budden, K. G. (1966), *Radio Waves in the Ionosphere*, p. 269, Cambridge University Press, London.

Carpenter, D. L. (1967), Relations between the dawn minimum in the equatorial radius of the plasmapause and *Dst*, *Kp*, and local *K* at Byrd Station, *J. Geophys. Res.*, *72*, 2969-2971.

Carpenter, D. L. (1968), Ducted whistler-mode propagation in the magnetosphere; A half-gyrofrequency upper intensity cutoff and some associated wave growth phenomena, *J. Geophys. Res.*, *73*, 2919-2928.

Dunckel, N., and R. A. Helliwell (1969), Whistler-mode emissions on the OGO 1 satellite, *J. Geophys. Res.*, *74*, 6371-6385.

Helliwell, R. A. (1965), *Whistlers and Related Iodospheric Phenomena*, Stanford University Press, Stanford, Ca.

Helliwell, R. A., J. P. Katsufrakis, and M. L. Trimpi (1973), Whistler-induced amplitude perturbation in VLF propagation, *J. Geophys. Res.*, *78*, 4679-4688.

Heyborne, R. L. (1966), Observations of whistler-mode signals in the OGO satellites from VLF ground station transmitters, *SEL-66-094*, Radioscience Laboratory, Stanford Electronics Laboratories, Stanford University, Stanford, Ca.

Heyborne, R. L., R. L. Smith, and R. A. Helliwell (1969), Latitudinal cutoff of VLF signals in the ionosphere, *J. Geophys. Res.*, *74*, 2393-2397.

International Telecommunication Union (1971), *International Frequency List, Vol. 1, 6th ed.*, International Telecommunication Union, Geneva, Switzerland.

Liemohn, H. B. (1967), Cyclotron-resonance amplification of VLF and ULF whistlers, *J. Geophys. Res.*, *72*, 39-55.

Smith, R. L. (1961), Propagation characteristics of whistlers trapped in field-aligned columns of enhanced ionization, *J. Geophys. Res.*, *66*, 3699-3707.

Walter, F. (1969), Nonducted VLF propagation in the magnetosphere, *Tech. Rep. No. 3418-1*, Radioscience Laboratory, Stanford Electronics Laboratories, Stanford University, Stanford, Ca.